Recl. Trav. Chim. Pays-Bas **114**, 387–394 (1995)
SSDI 0165-0513(95)00070-4

0165–0513/95/9/10 387-08$9.50

Molecular-mechanics and -dynamics simulations of trivalent europium complexes of calix[4]arene derivatives and a bislariat diazacrown ether

Frank C.J.M. van Veggel and David N. Reinhoudt

University of Twente, Faculty of Chemical Technology, Department of Organic Chemistry, P.O. Box 217, 7500 AE ENSCHEDE, The Netherlands
(Received March 3, 1995)

Abstract. Molecular-mechanics (MM) and molecular-dynamics (MD) simulations (in MeOH) were performed on Eu^{3+} complexes of two derivatized calix[4]arenes (**2b** and **2d**) and a bislariat diazacrown ether (**3**). The Quanta/CHARMm Lennard–Jones parameters of Ca^{2+} proved suitable as a model for the Lennard–Jones parameters of Eu^{3+}. The radial distribution function (RDF) of $Eu^{3+} \cdots$ MeOH (O) agrees well with experimental data. The MD of **2b** · Eu^{3+} showed that the phenolic oxygens cannot compete with the solvent, although they are preorganized. Three molecules of MeOH are within the first coordination shell. The MD of **2d** · Eu^{3+} showed two transitions. After the first the Eu^{3+} was coordinated by one molecule of MeOH and after the second by three molecules of MeOH. The pyridine ring was not involved in coordination to Eu^{3+}, which explained the measured lifetimes and derived coordination shells in methanol. The calculations on **3** · Eu^{3+} revealed that the conformation with the pendant arms in an *anti* configuration is unlikely to exist in solution, whereas the *syn* form calculated by MM rearranged to a structure with two molecules of MeOH in the first coordination sphere. This is consistent with experimental data, which show that the two dominant species in methanol solution have two molecules of MeOH coordinated to the Eu^{3+}. All calculations were performed with the Quanta/CHARMm package.

Introduction

One of our research topics is the synthesis of well-defined cation complexes having shielded cavities[1]. The calixspherand **1** (see Chart 1) is able to shield complexed alkali cations from the environment by providing a very hydrophobic exterior. This hydrophobic mantle prevents solvent molecules from assisting the decomplexation of the ion, which is the major reason for the kinetic inertness. The slow decomplexation rates of the Rb^+ complexes are particularly noteworthy, because these cannot be obtained with the Cram spherand[2]. It has been known for several years that luminescence of excited Eu^{3+}, and to a lesser extent Tb^{3+}, complexes can be increased by receptor molecules that strip off ligands such as water or methanol[3]. The OH oscillator is a very efficient quencher of the excited states of the above-mentioned cations.

Recently we have extended our work to trivalent cations and reported the synthesis and luminescence properties of the Eu^{3+} and Tb^{3+} complexes of the derivatized calix[4]arenes **2** shown in Chart 2[4]. The compounds **2a,c,d** have a ninth coordination site that can potentially increase the shielding, leading to improved luminescence properties, *i.e.* longer lifetimes. However, the experimental data (in MeOH solution) did not give any indication of improved luminescence properties with respect to **2b**. Approximately 1.5 ± 0.5 molecules of MeOH are in the first coordination sphere, according to the empirical relation of *Horrocks*[5]. This relation estimates the number of OH oscillators in the first coordination shell of Eu^{3+} from the radiative life-times of the $^5D_0$ state in MeOH and MeOD. For methanol this relation is: $n = 2.1 \cdot (\tau^{-1}_{MeOD} - \tau^{-1}_{MeOH})$. The luminescence properties of the Eu^{3+} and Tb^{3+} complexes of the calix[4]tetramide **2e**, that in contrast to the ligands **2a-d** is a neutral ligand, have been reported by *Ungaro* et al.[6]. They showed that approximately 1 ± 0.5 molecules of MeOH are bound to the ion in MeOH solution[6]. *Wipff* et al.[7] have calculated the structural properties of **2e** · Eu^{3+} in the gas phase, in water and in acetonitrile solution by molecular mechanics and molecular dynamics simulations. Some of their results are included in the discussion of our results.

We[8] and others[9] have reported MM studies on tetrahydroxy and tetramethoxy calix[4]arenes that agree reasonably well with experimental data. Recently we have calculated all reaction pathways of the conformational interconversions that are possible in (derivatized) calix[4]arenes[10], using the Conjugate-Peak-Refinement (CPR) algorithm in CHARMm. The calculated activation energies are in excellent agreement with experimental data. The activation energies of the rotation of DMF, DMA, and NMP in calix[4]arene-based carceplexes were also correctly calculated[11].

The following aspects will be addressed in this paper. The first problem is which model to use to mimic trivalent cations. *Fossheim* and *Dahl* have published non-bonded parameters for Gd^{3+}, which were fitted to the crystal structure of EuDOTA · H_2O[12], and we have used similar parameters. A second question concerns the force field. In order to study the quality of the CHARMm force field, the Eu^{3+} complex of the bislariat diazacrown ether **3** (Chart 3) was studied, because this complex has been well characterized by *Horrocks* and co-workers[13]. An important observation was that the deconvolution of the emission line around 580 nm of the non-degenerated $^5D_0$–$^7F_0$ transition showed the presence of three species in MeOH

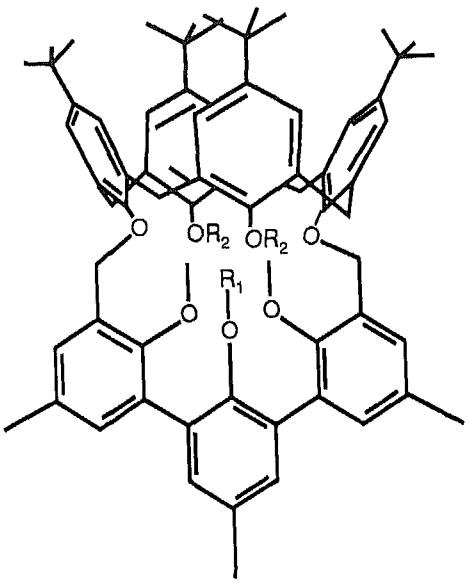

1

R_1	R_2
CH_3	CH_3
CH_2CH_3	CH_3
$CH(CH_3)_2$	CH_3
CH_3	CH_2CH_3

solution. The species that emits at 579.37 nm has 3 molecules of MeOH bound and the other two which emit at 579.96 and 580.10 nm, respectively, both have 2 molecules of MeOH coordinated. To our knowledge **3** · Eu^{3+} has not been studied by computational techniques, although simulations on related complexes of terlariat and hexakis-polyazacrown ethers have appeared[14]. The gas-phase minimizations showed that coordination of water molecule(s) is possible, although constraints on the Eu(3+)···O_{water} have to be imposed in order to prevent rearrangements of the ligands with subsequent removal of water molecules from the first coordination shell. The

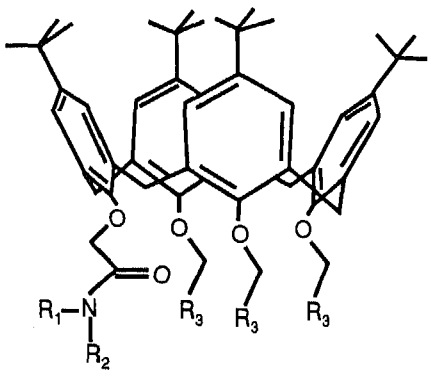

2a·3H R_1= H, R_2= $(CH_2)_2NHC(O)Me$, R_3= COOH
2b·3H R_1= H, R_2= n-Pr, R_3= COOH
2c·3H R_1= H, R_2= $(CH_2)_2$-2-Py, R_3= COOH
2d·3H R_1= H, R_2= CH_2-2-Py, R_3= COOH
2e R_1= R_2= Et, R_3= $C(O)NEt_2$

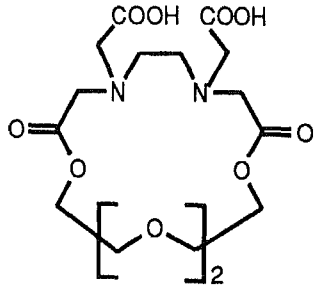

3·2H

third aspect relates to the coordination shell of the lanthanide complexes of **2a-d**. Can the essentially similar luminescence properties be rationalised by computer simulations? The last point that deserves attention is the dynamic behaviour of the trivalently negatively charged ligands **2a-d** compared to that of the neutral ligand **2e**.

The treatment of long-range (electrostatic) interactions is still a matter of discussion in the literature[15]. In principle, the non-bonded parameters are dependent on how the long-range interactions are treated. The cut-off distance is important and also what kind of cut-off is applied. That is, a "sharp" cut-off can be used but also a switch or shift function. *Lau* et al.[15b] have shown that the influence of the truncation method (*i.e.* a sharp cut-off, a switching function, or using the Ewald summation) on the RDF is rather moderate. Another factor that influences the parameters is the use of periodic boundaries or the Born correction[16]. By using a large cut-off radius of 14 Å we can assume that serious artefacts will be prevented (*vide infra*). *Tasiki* et al.[15c] have stipulated that if an atom-based list is used for the non-bonded interactions, a cut-off distance of larger than 12 Å has to be used in order to minimize artefacts. When dealing with trivalent cations electronic polarization effects are likely to be important, but current force fields cannot handle these.

Experimental

Initial structures as well as visualizations were carried out with Quanta 3.3[17]. The MM and MD calculations were run with CHARMm 22.0[18], as implemented in the Quanta/CHARMm package. Parameters were taken from Quanta 3.3 and point charges were calculated with the charge-template option in Quanta. The carboxylate oxygen atoms were symmetrically charged with −0.60 e. Ligands **2b** and **2d** were charged to −3 and ligand **3** to −2, with a small "excess" charge smoothed to non-polar carbons and hydrogens. The europium cation was represented as a calcium ion with a point charge of +3. The Lennard–Jones parameters of Ca^{2+} (R_{min} = 1.744 Å and ϵ = −0.060 kcal/mol) were taken for reasons outlined in the Results and Discussion sections. The starting structures were minimized by adopted-basis set Newton–Raphson (ABNR) until the RMS of the energy gradient was < 0.001 kcal·mol^{-1}·Å^{-1}. No cut-off on the non-bonded interactions was applied. A distant-dependent dielectric constant was used.

Details of the MD simulations are as follows. The minimized complexes were dissolved in a cubic methanol box of 30.747 Å dimensions, filled with 429 OPLS MeOHs[19] to give the correct density at 25°C. Solvent molecules that overlap with the complexes were removed (based on heavy atom interatomic distances $\leq$ 2.3 Å). Full periodic boundary conditions were imposed. Before running the MD simulation the system was minimized by 500 cycles steepest descent followed by ABNR until the RMS on the energy gradient was $\leq$ 0.01 kcal·mol^{-1}·Å^{-1} or a maximum of 1000 steps was reached. During the MD simulation the non-bonded list was updated every 20 time steps with a cutoff of 14 Å. The Van-der-Waals interactions were treated with the switch function between 10 and 13 Å, whereas the

shift function was applied to the electrostatic interactions. A constant dielectric constant and an ϵ of 1 were used. The system was heated to 300K in 5 ps, followed by 10 ps of equilibration with scaling of velocities within a temperature window of $\pm 10°$. After equilibration no scaling of velocities was applied. The production phase consisted of 50 to 150 ps, depending on the system under investigation, and coordinates were saved every 200 time steps. For the numerical integration the verlet/leapfrog algorithm was applied. The SHAKE algorithm[20] on bonds involving hydrogen was used, allowing a time step of 1 fs.

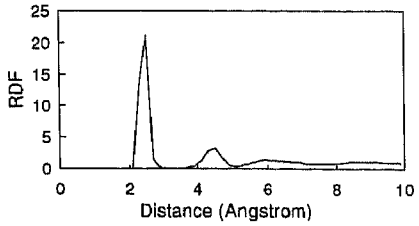

Figure 1. RDF of Eu^{3+}–MeOH (O).

Results and discussion

1. The non-bonded parameters for Eu^{3+}

Before running MM and MD simulations of the complexes the Lennard–Jones parameters of Ca^{2+} (R_{min} = 1.744 Å and $\epsilon = -0.060$ kcal/mol) were tested as a model for a trivalent lanthanide ion, because Ca^{2+} and Ln^{3+} complexes are very often iso-structural[21]. An MD simulation of the trivalent ion was carried out in a periodic cubic box of OPLS MeOH of 30.747 Å dimension[19]. After heating and equilibration, 50 ps of production were calculated, which were used to calculate the RDF of oxygens around the Eu(3 +) ion. Figure 1 shows the first coordination sphere around the ion at approximately 2.3 Å. This peak integrates to about 7.5 oxygens, which corresponds well with the experimental value of 7.1 ± 0.5 determined by *Horrocks* and co-workers[13]. The second coordination sphere is centered at approximately 4.3 Å and is also quite distinct. This is not very surprising since the electrostatic interactions involving a trivalent cation are long ranged. The RDF of Eu^{3+}–MeOH (C) shows the first and second coordination spheres at approximately 3.4 and 5.0 Å, respectively (data not shown). Beyond 8 Å, no specific features were found and we conclude that a cut-off radius of 14 Å should be sufficient to prevent

Table I (Interaction) energies of the minimized structures in kcal / mol.

	E_{sum}	E_{el}	E_{VdW}	E_{bond}	E_{angle}	E_{dihe}	E_{impr}
2b·Eu^{3+} E_{total}	−336.6	−398.2	8.0	3.4	13.8	33.4	2.9
E_{host}	80.8	55.0	−27.8	3.4	13.8	33.4	2.9
$E_{interaction}$ [a]	−417.4	−453.2	35.8				
2d·Eu^{3+} E_{total}	−356.2	−442.7	30.7	4.4	18.2	30.3	2.9
E_{host}	89.9	59.2	−25.1	4.4	18.2	30.3	2.9
$E_{interaction}$ [a]	−446.1	−501.9	55.8				
3·Eu^{3+}, *anti*							
E_{total}	−420.4	−515.9	48.7	2.3	13.1	23.6	7.9
E_{host}	104.5	68.6	−11.0	2.3	13.1	23.6	7.9
$E_{interaction}$ [a]	−524.8	−584.5	59.7				
3·Eu^{3+}, *syn*							
E_{total}	−415.7	−516.2	52.8	3.3	14.5	20.6	9.2
E_{host}	103.9	65.1	−8.8	3.3	14.5	20.6	9.2
$E_{interaction}$ [a]	−519.6	−581.2	61.7				
3·$Eu^{3+}Cl^-$, *anti*							
E_{total}	−460.4	−545.8	49.5	3.0	13.0	16.2	3.7
E_{host}	101.6	71.7	−6.1	3.0	13.0	16.2	3.7
$E_{interaction}$ [a]	−506.8	−550.9	44.2				
$E_{interaction}$ [b]	−111.0	−117.2	6.2				
$E_{interaction}$ [c]	55.8	50.7	5.2				
$E_{interaction}$ [d]	−55.2	−66.6	11.4				
3·$Eu^{3+}Cl^-$, *syn*							
E_{total}	−452.5	−544.3	59.0	2.1	11.0	16.0	3.7
E_{host}	60.0	37.8	−10.7	2.1	11.0	16.0	3.7
$E_{interaction}$ [a]	−447.8	−503.1	55.3				
$E_{interaction}$ [b]	−118.3	−131.8	13.5				
$E_{interaction}$ [c]	53.7	52.8	0.9				
$E_{interaction}$ [d]	−64.6	−79.0	14.3				

[a] Interaction energy host and Eu^{3+}. [b] Interaction energy Eu^{3+} and Cl^-. [c] Interaction energy host and Cl^-. [d] Interaction energy L·Eu^{3+} and Cl^-.

Table II Coordination distances of minimized structures in Å.

Compound	PhO	COO^-	$C{=}O_{amide}$	N	O_{ester}	O_{ether}	Cl^-
2b·Eu^{3+}	2.53–2.90	2.27–2.31	2.31	–	–	–	–
2d·Eu^{3+}[a]	2.41–2.75	2.23–2.24	2.20	–	–	–	–
3·Eu^{3+}, *anti*	–	2.31–2.35 [b]	–	3.06, 3.09	2.35, 2.40	2.35, 2.38	–
3·Eu^{3+}, *syn*	–	2.34–2.40 [b]	–	2.91, 3.01	2.30, 2.31	2.32, 2.36	–
3·$Eu^{3+}Cl^-$, *anti*	–	2.33–2.46 [b]	–	3.45, 3.51	2.38, 2.47	2.38, 2.47	2.92
3·$Eu^{3+}Cl^-$, *syn*	–	2.27–2.32 [b]	–	3.36, 4.19	2.36, 5.27	2.43, 4.48	2.75

[a] $Eu^{3+} \cdots NPy = 3.26$ Å.
[b] Both oxygens of a carboxylate group are coordinated.

Table III Averaged coordination distances and standard deviation (in parentheses) in Å in the MD simulations.

Compound	PhO	COO^-	$C{=}O_{amide}$	N	O_{ester}	O_{ether}	Cl^-
2b·Eu^{3+}	4.32–4.52 (0.10–0.12)	2.26–2.52 (0.07–0.20)	2.34 (0.07)	–	–	–	–
2d·Eu^{3+} [a]				–	–	–	–
10–45 ps	2.56–2.97 (0.10–0.17)	2.25–2.26 (0.04–0.05)	2.21 (0.05)	–	–	–	–
50–100 ps	4.17–4.46 (0.12–0.14)	2.26–2.33 (0.05–0.07)	2.27 (0.06)				
3·Eu^{3+}, *anti*	–	2.31–2.39 (0.06–0.09) [b]	–	3.33(0.12), 3.30(0.11)	2.40(0.08), 2.47(0.12)	2.39(0.07), 2.48(0.08)	–
3·Eu^{3+}, *syn*	–	2.28–2.37 (0.05–0.06) [b]	–	3.29(0.11), 4.36(0.11)	2.34(0.08), 5.25(0.21)	2.40(0.08), 4.42(0.18)	–
3·$Eu^{3+}Cl^-$, *anti*	–	2.34–2.46 (0.07–0.13) [b]	–	3.43(0.12), 3.47(0.11)	2.43(0.09), 2.48(0.11)	2.40(0.06), 2.49(0.08)	2.83 (0.07)
3·$Eu^{3+}Cl^-$, *syn*	–	2.29–2.33 (0.05–0.07) [b]	–	3.42(0.11), 4.42(0.10)	2.39(0.08), 5.34(0.18)	2.42(0.08), 4.52(0.16)	2.78 (0.05)

[a] $Eu^{3+} \cdots NPy$ = 4.84 (0.30) Å (10–45 ps) and 5.40 (0.56) Å (50–100 ps).
[b] Both oxygens of the carboxylate group are coordinated.

artefacts by the cut-off. This simulation proves that the Lennard-Jones parameters of Ca^{2+} are suitable for the purpose of our studies, which is to obtain structural information.

2. The monovalently charged complex of 3 · Eu^{3+}

The ligand **3** · 2H can in principle occur in two major conformations, *i.e.* a conformation with the two side-arms *syn* and another with the two side-arms *anti* with regard to the plane of the macrocycle. Both monovalently charged Eu^{3+} complexes of **3** were generated and minimized *in vacuo*. Figure 2 shows the structures of the two conformations with the lowest energy (Table I) and in both the Eu^{3+} is well shielded by the donor atoms, which are all within the first coordination shell (Table II). The total energy of *anti* **3** · Eu^{3+} is lower than of *syn* **3** · Eu^{3+} by 4.7 kcal/mol mainly due to a more favorable interaction energy between the ligand and the Eu^{3+}. The complex of the *anti* conformation shows unusual coordination by the carboxylate groups, not only the two oxygen atoms but also the carbon atoms are within the first coordination shell of Eu^{3+}. From the space-filling representation of *anti* **3** · Eu^{3+}, it is obvious that the ligand cannot accommodate the Eu^{3+} in such a way that the carboxylate groups behave as mono- or true bidentate ligands. Several runs with monodentate carboxylate groups resulted in the binding fashion shown in Figure 2a. The complex of the *syn* orientation is presented in Figure 2b in which the two carboxylate groups act as bidentate ligands.

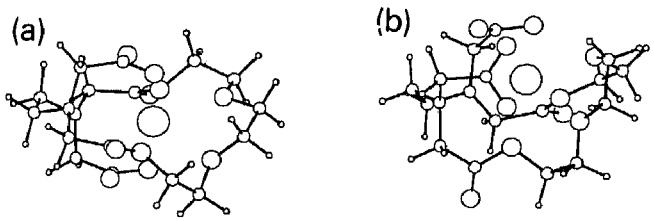

Figure 2. Minimized structures of 3·Eu^{3+} (a) side-arms in anti *orientations and (b) side-arms in* syn *orientations.*

MD runs of both minimized structures were carried out in MeOH for 150 ps each. The sum of the averaged energies of the complex and the interaction energy of the complex with the solvent are -1034 ± 12 and -1057 ± 12 kcal/mol for the *anti* and *syn* form, respectively, showing that the *syn* form is the more stable. Some of the aver-

Table IV Averaged (interaction) energies and standard deviations (in parentheses) in kcal / mol in the MD simulations [a].

Compound	E ligand	E complex	E complex Cl^-	E_{int} Eu^{3+}–ligand	E_{int} Eu^{3+}–Cl^-	E_{int} ligand–Cl^-	E_{int} complex–Cl^-	E_{int} Eu^{3+}–solvent	E_{int} Ligand–solvent	E_{int} complex–solvent	E_{int} complex–Cl^-–solvent	E_{int} Cl^-–solvent
2b·Eu^{3+}	307(11)	−649(9)	–	−957(10)	–	–	–	−334(18)	−82(18)	−416(14)	–	–
2d·Eu^{3+}												
10–45 ps	292(10)	−705(8)	–	−996(9)	–	–	–	−103(17)	−151(18)	−254(11)	–	–
50–100 ps	310(10)	−644(9)	–	−953(10)	–	–	–	−302(19)	−125(19)	−427(16)	–	–
3·Eu^{3+}, *anti* [b]	226(10)	−835(6)	–	−1062(11)	–	–	–	−193(23)	−6(23)	−199(12)	–	–
3·Eu^{3+}, *syn* [c]	181(10)	−788(7)	–	−969(10)	–	–	–	−304(21)	36(17)	−269(12)	–	–
3·$Eu^{3+}Cl^-$, *anti*	288(11)	−822(7)	−963(5)	−1050(12)	−310(6)	169(6)	−141(6)	55(19)	−159(18)	−104(11)	−144(10)	−40(8)
3·$Eu^{3+}Cl^-$, *syn*	180(9)	−784(6)	−937(5)	−937(9)	−315(4)	161(4)	−154(5)	−38(18)	−108(15)	−146(11)	−170(10)	−25(8)

[a] E_{int} is the interaction energy. [b] E_{int} L·Eu^{3+}–$MeOH_{coord}$ = −37(3) kcal/mol; E_{int} $MeOH_{coord}$–remaining-solvent = −11(2) kcal/mol. [c] E_{int} L·Eu^{3+}–$MeOH_{coord}$ = −88(3) kcal/mol; E_{int} $MeOH_{coord}$–remaining-solvent = −16(3) kcal/mol. [d] E_{int} L·Eu^{3+}–$MeOH_{coord}$ = −43(3) kcal/mol; E_{int} $MeOH_{coord}$–remaining-solvent = −13(2) kcal/mol; $E_{int}Cl^-$–$MeOH_{coord}$ = 12(2) kcal/mol.

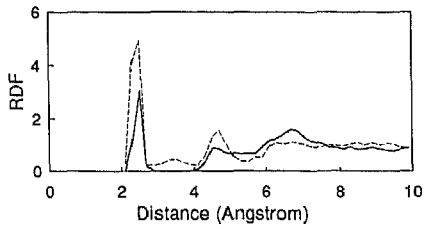

Figure 3. RDF of Eu^{3+}–MeOH (O) of anti *3·Eu^{3+} (———) and* syn *3·Eu^{3+}.(– – – – –)*

aged distances and (interaction) energies are summarized in Tables III and IV, respectively. The RDF of anti **3** · Eu^{3+} and the oxygen of MeOH (Figure 3) shows the first coordination around 2.3 Å, and this integrates to about 1.0 oxygen. Some weak long-range features are observed. A typical structure of this monosolvated Eu^{3+} complex is presented in Figure 4a. The Eu^{3+} has moved from the macrocycle towards the solvent, which is reflected in the somewhat longer coordination distances of the nitrogen atoms and the ester and ether oxygen atoms. The two carboxylate group behave as bidentate ligands. It is clear from this MD run that minimization in vacuo results in an overestimation of the shielding. The structure of *anti* **3** · Eu^{3+} in MeOH is not consistent with the reported data[13] (*vide supra*) and is therefore unlikely to exist.

The RDF of *syn* **3** · Eu^{3+} and the oxygen of MeOH is shown in Figure 3 and has a first coordination peak centered at 2.3 Å that integrates to approximately 2.0 oxygens. Relatively strong long-range features are observed, which is probably due to the fact that in the *syn* conformation the Eu^{3+} is more exposed to the solvent and therefore the charge is not as well (partially) compensated as in the *anti* conformation (Figure 4b). The Eu^{3+} moves away from the macrocycle compared to the structure minimized *in vacuo* (Tables II and III). The experimental data for the transitions at 579.98 and 580.09 nm both correspond to structures with 2.0 ± 0.5 molecules of MeOH bound to the Eu(3 +), and the *syn* conformation of $3Eu^{3+}$ agrees well with such a structure (*vide supra*). The small difference in the two wavelengths is most likely due to a subtle difference in the crystal field and we thought it fruitless to search for two such similar structures in our simulations. These results show that the CHARMm force field in combination with the OPLS MeOH parameters provides a good model.

3. Anion binding to 3 · Eu^{3+}

Wipff and co-workers[7] have emphasized that the binding of anions like Cl^- to complexes with an overall positively charge may play an important role in the structure of the complexes. Therefore, both *anti* and *syn* 3 · $Eu^{3+}Cl^-$ were generated and minimized *in vacuo*, followed by MD

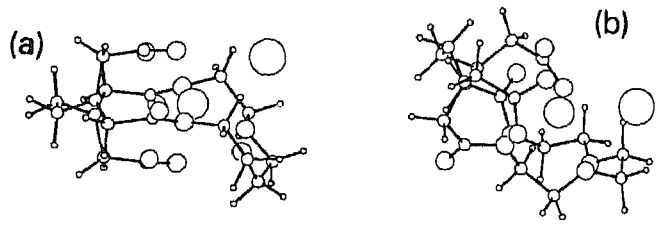

Figure 5. Minimized structure of 3·$Eu^{3+}Cl^-$ (a) anti *conformation, (b)* syn *conformation.*

in MeOH. The minimized structures (Figure 5) and the coordination distances (Tables I and II) show that the *anti* conformation is more stable than the *syn* conformation. The Van-der-Waals interactions are more favorable for the *anti* conformation than the *syn* conformation and the electrostatic contributions are almost the same. In both MD simulations the chloride remains coordinated to the europium ion, although the interaction between the ligand and the chloride is unfavorable due to the close proximity of negatively charged coordinating carboxylate and other oxygen atoms. In the *anti* conformation no space in the first coordination shell of the lanthanide is left for solvent molecules. The RDF of Eu^{3+}–MeOH (O) shows no features below 4 Å (Figure 6) although the typical long-range features around 5 and 7 Å are present. The RDF of the chloride–MeOH (H) shows a peak around 2.5 Å, that integrates to approximately 1.5 molecules of MeOH (Figure 6). Comparison of the coordination distances in Tables II and III shows that no significant conformational changes in *anti* **3** · $Eu^{3+}Cl^-$ occurs during the MD run. This behavior was also observed for the *syn* conformation. The interaction energy of the Eu^{3+} and the solvent is only unfavorable for *anti* **3** · $Eu^{3+}Cl^-$ (Table IV). Visual inspection of various saved coordinates of the MD shows that in the first coordination shell mainly hydrogens and methyl groups of the solvent are present. They have a favorable interaction with the ligand and chloride and, of course, an unfavourable interaction with the Eu^{3+}. The coordination of the chloride in the *syn* conformation allows one molecule of methanol to enter the first coordination sphere of the lanthanide ion. The RDF of Eu^{3+}–MeOH (O) (Figure 6) shows one peak at ≈ 2.3 Å that integrates to about one oxygen. The RDF of chloride–MeOH (H) shows a first peak around 2.5 Å that integrates to about one hydrogen of MeOH (Figure 6). The fact that now only one hydrogen bond is formed is reflected in a less favorable interaction energy between the chloride and the solvent compared to the *syn* conformation (−24.7 *vs.* −40.1 kcal/mol, respectively).

The overall conformations of solvated *anti* **3** · Eu^{3+} and *anti* **3** · $Eu^{3+}Cl^-$ and of the bisolvated *syn* **3** · Eu^{3+} and monosolvated *syn* **3** · $Eu^{3+}Cl^-$ (see Tables III and IV) are quite similar. Apparently the difference between a

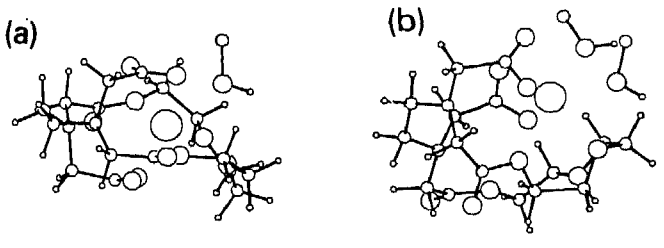

Figure 4. Typical structure from the MD simulations of (a) the anti *3·Eu^{3+} complex with one coordinated MeOH and (b)* syn *3·Eu^{3+} complex with two coordinated MeOHs.*

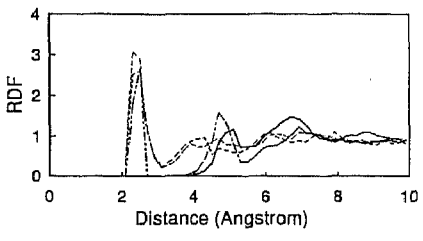

Figure 6. RDF of Eu^{3+}–MeOH (O) of anti *3·Eu^{3+}(———), Cl^-–MeOH (H) of* anti *3·$Eu^{3+}Cl^-$(– – – – –), and Eu^{3+}–MeOH (O) of* syn *3·$Eu^{3+}Cl^-$(– · ·) and Cl^-–MeOH (H) of* syn *3·$Eu^{3+}Cl^-$ (···).*

coordinated chloride and a coordinated molecule of methanol is very small. Comparison of the minimized structures and the averaged structures in the MD (Tables II and III, respectively) shows that the solvent does not induce a significant conformational change. This is also seen in the energies of the two sets of complexes of $\mathbf{3}\cdot Eu^{3+}$ and $\mathbf{3}\cdot Eu^{3+}Cl^-$ (−835, −822 and −788, −784 kcal/mol; Table IV). As expected, the solvation energies of *anti* and *syn* $\mathbf{3}\cdot Eu^{3+}$ are larger than of *anti* and *syn* $\mathbf{3}\cdot Eu^{3+}Cl^-$, but this loss is more than compensated by the interaction between the complex and the chloride. The sum of the energies of $\mathbf{3}\cdot Eu^{3+}Cl^-$ and the interaction energy with the solvent for both the *anti* and *syn* conformation are identical (-1107 ± 12 kcal/mol) and more negative than the two complexes without the chloride. We can draw two conclusions from these simulations which include the counter-anion. Firstly, the europium chloride complexes, although energetically more stable, are not consistent with the experimental data from *Horrocks* and co-workers[13]. They are apparently thermodynamically less stable. Therefore, it is unlikely that anion binding to overall monovalently charged complexes is important. The difference in the thermodynamical stabilities of $\mathbf{3}\cdot Eu^{3+}$ and $\mathbf{3}\cdot Eu^{3+}Cl^-$ can in principle be calculated from a thermodynamic cycle with free energy perturbations: $\Delta G_1 = \Delta G_2 - \Delta G_3$ (see Eqn. 1). The free energies ΔG_2 and ΔG_3 are computationally accessible.

$$\begin{array}{lll} \mathbf{3}\cdot Eu^{3+}Cl^- & \xrightarrow{\Delta G_1} & \mathbf{3}\cdot Eu^{3+} + Cl^- \\ \downarrow \Delta G_2 & & \downarrow \Delta G = 0 \;\; \downarrow \Delta G_3 \\ \mathbf{3}\cdot Eu^{3+}\cdot \text{Dummy} & \xrightarrow{\Delta G = 0} & \mathbf{3}\cdot Eu^{3+} + \text{Dummy} \end{array} \qquad (1)$$

Secondly, on the assumption that the complexes without a coordinated chloride are thermodynamically not stable, even simulations of 150 ps are apparently not long enough to observe the diffusion of the chloride into the bulk of the solvent. In other words, the energy barrier to break the $\mathbf{3}\cdot Eu^{3+}$–Cl^- bond could apparently not be surmounted.

4. Overall neutral complexes of Eu^{3+}

The minimized structure *in vacuo* of the overall neutral $\mathbf{2b}\cdot Eu^{3+}$ is shown in Figure 7a. The four phenolic oxygens, the three carboxylate group, and the amide oxygen are coordinating the Eu^{3+} in an approximately cubic geometry (Table II). It is obvious from this structure that complete shielding of the cation from solvent molecules does not occur. The RDF, calculated from a 50-ps MD, of MeOH (O) around the Eu^{3+} of this complex (Figure 8) shows the first coordination sphere around 2.3 Å that integrates to about 3 oxygens. During the equilibration the cation moves from the phenolic oxygens towards the solvent. A typical structure (Figure 9) clearly shows that the cation is exposed to the solvent. It can be concluded that the oxygens of MeOH are more competitive that the phenolic oxygens mainly due to a larger charge (O_{MeOH} −0.70 and PhO −0.23, respectively)[17,19]. A similar exposure of the cation to the solvent has also been observed by *Wipff* et al. in a simulation of $\mathbf{2e}\cdot Eu^{3+}$ in water[7a]. During our 50-ps MD simulation the coordination distances of the three carboxylate oxygens and the amide oxygen remained well within the first coordination shell. Hydrogen bonds between the solvent and the carboxylate oxygens that are not coordinated to the europium ion are frequently formed. The amide proton is involved in hydrogen bonding to the methanol oxygen atoms. The cavity at the upper rim of the calix is filled with one molecule of methanol. At the start of the simulation the oxygen atom of this methanol is deeply penetrated in the cavity and has

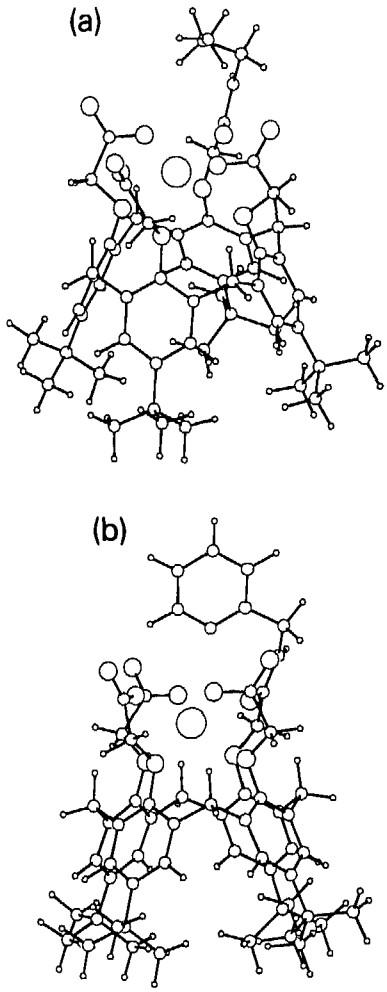

Figure 7. Minimized structure of (a) $\mathbf{2b}\cdot Eu^{3+}$ and (b) $\mathbf{2d}\cdot Eu^{3+}$.

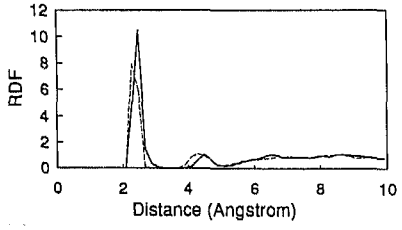

Figure 8. RDF of Eu^{3+}–MeOH (O) of $\mathbf{2b}\cdot Eu^{3+}$ (———) and Eu^{3+}–MeOH (O) of $\mathbf{2d}\cdot Eu^{3+}$ after second transition (-----).

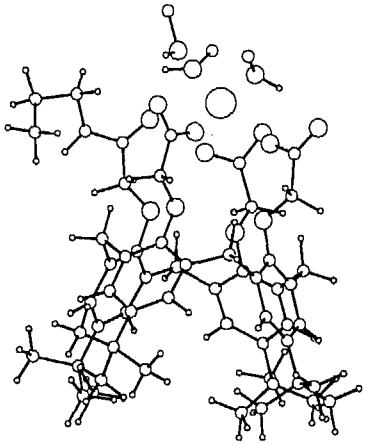

Figure 9. Typical structure from the MD simulation of (a) $\mathbf{2b}\cdot Eu^{3+}$ with the cation coordinated to 3 MeOHs.

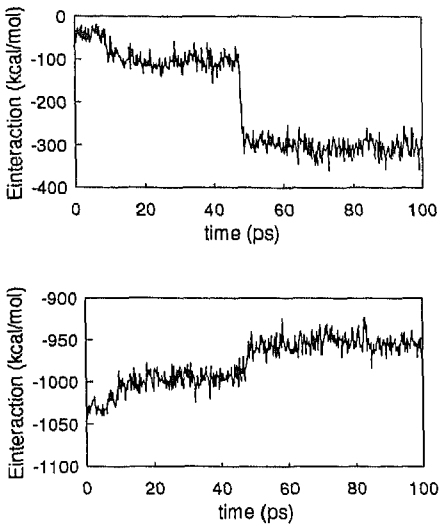

Figure 10. Interaction energy of **2d** · Eu^{3+} *and the solvent* versus *time (top) and interaction energy of ligand* **2d** *and* Eu^{3+} versus *time (bottom).*

a favorable interaction with the europium ion (approximate distance 3.5 Å). In the equilibration phase the europium ion moves towards the solvent and this reduces the penetration of the methanol into the cavity. The oxygen atom of MeOH becomes exposed to the rest of the solvent and the hydrogen of MeOH has an interaction with the π surface of one of the four phenyl rings. The methyl group is still in the hydrophobic cavity. The inclusion of methanol in the hydrophobic cavity of calix[4]arenes has been observed in the X-ray structure of **2e** · KI and **2e** · KSCN[22]. The oxygen atom of MeOH is most deeply in the cavity. This means that our results are in agreement with the available experimental data. The minimized structure *in vacuo* of **2d** · Eu^{3+} with a ninth coordination site is shown in Figure 7b, in which the cation is well shielded from the environment. The coordination distances of the four phenolic oxygens, the three carboxylate groups, and the amide oxygen are very similar to those of **2b** · Eu^{3+} (see Table II). The coordination distance between the pyridine nitrogen and Eu^{3+} is 3.26 Å and is somewhat long compared to the other eight distances. This greater distance is due to a relatively short spacer between the amide nitrogen and the pyridine ring. The additional coordination is reflected in an increased electrostatic interaction energy between the Eu^{3+} and the ligand compared to **2b** · Eu^{3+} (−446.1 and −417.4 kcal/mol, respectively). The 100-ps MD simulation of **2d** · Eu^{3+} in MeOH shows two transitions, one at approximately 10 ps and the other at approximately 48 ps (Figure 10). The interaction energy between the complex and the solvent increases at both transitions, whereas the interaction energy of the ligand and Eu^{3+} decreases at both transitions. The RDF of Eu^{3+} and MeOH (O) after the first transition has a first coordination sphere centered at ≈ 2.3 Å that integrates to about 1 oxygen (data not shown). The RDF of Eu^{3+} and MeOH (O) after the second transition (Figure 8) shows a peak centered at 2.3 Å that integrates to about 3 oxygens and resembles that of **2b** · Eu^{3+}. The averaged coordination distances are given in Table III which mark the progressive displacement of the Eu^{3+} from the phenolic oxygens. Only the first transition is observed in a plot of the coordination distance of the pyridine nitrogen and the Eu^{3+} *versus* time. Typical structures of the 10–45 and 50–100 ps time windows are shown in Figure 11. After the second transition the Eu^{3+} is exposed mostly to the solvent. The behavior of the MeOH in the hydrophobic cavity is similar to that described for **2b** · Eu^{3+} (*vide supra*). The hydrogen-bonding behavior of the non-europium-coordinated carboxylate oxygens and the amide proton also follow the same pattern as found for **2b** · Eu^{3+}. According to the calculated RDF of the nitrogen atom of the pyridine ring and MeOH (H) the nitrogen is not involved in hydrogen bonding (data not shown). The reason is that the solvent-orienting effect of the trivalent europium ion is so strong that it dominates the solvent structure. Comparison of the energies of the ligand, the energies of the complex, and the interaction energies between ligand and Eu^{3+} of **2b** · Eu^{3+} and **2d** · Eu^{3+} (Table IV) shows that the differences between a solvated *n*-propyl and CH_2-2-Py group are only marginal. The somewhat larger interaction energy between **2d** · Eu^{3+} and the solvent is apparently due to the fact that the CH_2-2-Py group is larger than the *n*-propyl group and not to a hydrogen bond to the pyridine nitrogen. The fact that the interaction energy of Eu^{3+} and the solvent is less favorable for **2d** · Eu(3 +) than for **2b** · Eu^{3+} can be explained by the fact that the larger substituent of the amide group blocks more solvent molecules than a *n*-propyl group. From this simulation it is obvious that the pendant arm, with a possible coordination site, is not efficient at shielding the cation from the solvent. The fact that **2b** · Eu^{3+} and **2d** · Eu^{3+} gave similar structures and hence RDFs explains the observed similar experimentally determined lifetimes[4]. The number

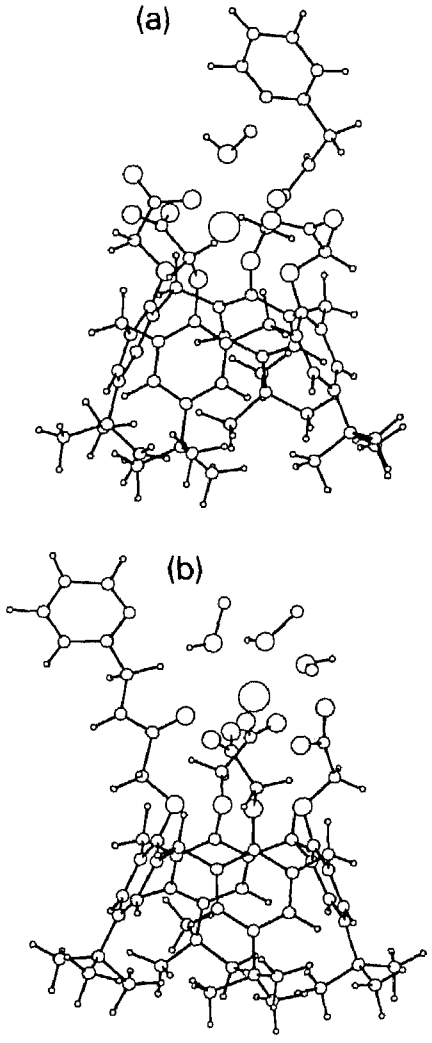

Figure 11. Typical structure from the MD simulation of **2d** · Eu^{3+} *after (a) the first transition and (b) the second transition.*

of MeOHs in the first coordination sphere is overestimated by 1 (3 *versus* 2, respectively) but this is not necessarily an artefact of the simulations. It is well known that small amounts of non-deuterated methanol or water in perdeuterated methanol have a large effect on the observed lifetimes[3] and dissolution of the hydrated complexes introduces small amounts of water and leads to hygroscopic solutions. A better shielding might be obtained with a more rigid spacer which forces the ninth coordinating atom to the Eu^{3+} and possibly by an additional carboxylate group which is known to have the strongest interaction with the Eu^{3+}.

The Eu^{3+} complex of **2e** has been studied by *Wipff* and co-workers by MM and MD in water and acetonitrile[7]. The MD simulation in water also shows a transition in which the Eu^{3+} moves from the phenolic oxygens towards the water. The calculated RDF ($Eu^{3+} \cdots O_w$) shows a peak at 2.3 Å that integrates to approximately 4 water oxygens. One molecule of water is nested between the Eu^{3+} and the phenolic oxygens. The other three are at the opposite face of the Eu^{3+}. Our results of the MDs on **2b** and **2d** in MeOH are quite similar to that of **2e** in water, which means that the shielding properties of carboxylate and amide groups are quite similar.

Comparing the interaction energies of the Eu^{3+} with the solvent and the ligand with the solvent of the various complexes (Table IV) indicates that conformational changes are induced by Eu^{3+}–MeOH interactions.

Conclusions

The Lennard–Jones parameters of Ca^{2+} ($R_{min} = 1.744$ Å and $\epsilon = -0.060$ kcal/mol) are useful as a model for Eu^{3+} in MeOH solution. The identification of the major conformation of $\mathbf{3} \cdot Eu^{3+}$ in methanol solution with two molecules of MeOH in the first coordination sphere shows that the CHARMm force field is realistic. Simulations with coordinated chloride ions to $\mathbf{3} \cdot Eu^{3+}$ shows that counter-anion binding does not play a role in methanol solution. The simulation studies of $\mathbf{2b} \cdot Eu^{3+}$ and $\mathbf{2d} \cdot Eu^{3+}$ revealed that the pyridine nitrogen atom of the pendant arm does not increase the shielding of the europium ion. This provides an explanation for the similar lifetimes and coordination shells in methanol, determined by luminescent measurements. The overall conclusion is that MD simulations in solution provide a powerful tool for structural information, while MM calculations can be very misleading, because in general they overestimate shielding. Competing polar solvent molecules are not present and every possible coordination to a donor atom of the ligand will normally lower the total energy of the system.

References and notes

[1a] *W.I. Iwema Bakker, M. Haas, H.J. Den Hertog, Jr., W. Verboom, D. De Zeeuw, A.P. Bruins* and *D.N. Reinhoudt*, J. Org. Chem. **59**, 972 (1994);

[b] *W.I. Iwema Bakker, M. Haas, C. Khoo-Beattie, R. Ostaszewski, S.M. Franken, H.J. Den Hertog, Jr., W. Verboom, D. De Zeeuw, S. Harkema* and *D.N. Reinhoudt*, J. Am. Chem. Soc. **116**, 123 (1994).

[2a] *D.J. Cram*, Angew. Chemie **100**, 1041 (1988);

[b] *D.J. Cram*, Science **240**, 760 (1988).

[3] *N. Sabbatini, M. Guandigli* and *J.-M. Lehn*, Coord. Chem. Rev. **123**, 201 (1993).

[4] *D.M. Rudkevich, W. Verboom, E. Van der Tol, C.J. Van Staveren, F.M. Kaspersen, J.W. Verhoeven* and *D.N. Reinhoudt*, J. Chem. Soc., Perkin Trans. 2, 131 (1995).

[5a] *W. DeW. Horrocks* and *D.R. Sudnick*, J. Am. Chem. Soc. **101**, 334 (1979);

[b] ibid, Acc. Chem. Res. **14**, 384 (1981).

[6] *N. Sabbatini, M. Guandigli, A. Mecati, V. Balzani, R. Ungaro, E. Ghidini, A. Casnati* and *A. Pochini*, J. Chem. Soc., Chem. Commun. 878 (1990).

[7a] *P. Guilbaud, A. Varnek* and *G. Wipff*, J. Am. Chem. Soc. **115**, 8298 (1993);

[b] *A. Varnek* and *G. Wipff*, J. Phys. Chem. **97**, 10840 (1993).

[8a] *L.C. Groenen, J.A.J. Brunink, W.I. Iwema Bakker, S. Harkema, S.S. Wijmenga* and *D.N. Reinhoudt*, J. Chem. Soc. Perkin Trans. 2, 1899 (1992);

[b] *P.D.J. Grootenhuis, P.A. Kollman, L.C. Groenen, D.N. Reinhoudt, G.J. Van Hummel, F. Ugozzoli* and *G.D. Andreetti*, J. Am. Chem. Soc. **112**, 4165 (1990);

[c] *L.C. Groenen, J.-D. Van Loon, W. Verboom, S. Harkema, A. Casnati, R. Ungaro, A. Pochini, F. Ugozzoli* and *D.N. Reinhoudt*, J. Am. Chem. Soc. **113**, 2385 (1991).

[9a] *Y. Harada, J.M. Rudziński* and *S. Shinkai*, J. Chem. Soc., Perkin Trans. 2, 2109 (1992);

[b] *Y. Harada, J.M. Rudziński, E. Osawa* and *S. Shinkai*, Tetrahedron **49**, 5941 (1993).

[10] *S. Fischer, P.D.J. Grootenhuis, L.C. Groenen, W.P. Van Hoorn, F.C.J.M. Van Veggel, D.N. Reinhoudt* and *M. Karplus*, J. Am. Chem. Soc. **116**, 1611 (1995).

[11] *P. Timmerman, W. Verboom, F.C.J.M. Van Veggel, J.P.M. Van Duynhoven* and *D.N. Reinhoudt*, Angew. Chem., Int. Ed. Engl. **33**, 2345 (1994).

[12] *R. Fossheim* and *S.G. Dahl*, Acta Chem. Scan. **44**, 698 (1990).

[13] The Eu(3+) complex was prepared *in situ* from the **3**·2H and $EuCl_3$; *R.C. Holz, C.A. Chang* and *W. DeW. Horrocks, Jr.*, Inorg. Chem. **30**, 3270 (1991).

[14] *S.T. Frey, C.A. Chang, J.F. Carvalho, A. Varadarajan, L.M. Schultze, K.L. Pounds* and *W. DeW. Horrocks, Jr.*, Inorg. Chem. **33**, 2882 (1994).

[15a] *L. Perera, U. Essmann* and *M.L. Berkowitz*, J. Phys. Chem. **102**, 450 (1995);

[b] *K.F. Lau, H.E. Alper, T.S. Thacher* and *T.R. Stouch, J. Phys. Chem. 98, 8785 (1994);*

[c] *K. Tasaki, S. McDonald* and *J.W. Brady*, J. Comput. Chem. **14**, 278 (1993);

[d] *M. Saito*, J. Chem. Phys. **101**, 4055 (1994).

[16] *J. Aqvist*, J. Phys. Chem. **94**, 8021 (1990).

[17] Quanta was bought from Molecular Simulations Inc., Burlington, MA, USA.

[18] *B.R. Brooks, R.E. Bruccoleri, B.D. Olafsen, D.J. States, S. Swaminathan* and *M. Karplus*, J. Comput. Chem. **4**, 187 (1983).

[19] *W.L. Jorgensen*, J. Phys. Chem. **90**, 1276 (1986).

[20] *H.J.C. Berendsen, J.P.M. Postma, A. Di. Noia, W.F. van Gunsteren* and *J.R. Haak*, J. Chem Phys. **81**, 3684 (1984).

[21a] *W. DeW. Horrocks, Jr.*, Adv. Inorg. Biochem. **4**, 201 (1982);

[b] *J. Reuben*, in "Handbook on the Physics and Chemistry of Rare Earths", *K.A. Gschneidner* and *L. Eijring*, eds., North-Holland, Amsterdam, 1979, vol. 4, p. 515.

[22] *R. Ungaro, A. Arduini, A. Casnati, O. Ori, A. Pochini* and *F. Ugozzoli*, in "Computational Approaches in Supramolecular Chemistry", *G. Wipff*, ed., Kluwer Academic Publishers, Dordrecht, 1994, p. 277.